

AN ACCURATE 3D VISION SYSTEM USING A PROJECTED GRID FOR SURFACE GEOMETRICAL STUDY

Latifa GUISSER, René Payrissat and Serge CASTAN

IRIT, Université Paul Sabatier
118, route de narbonne
31062 TOULOUSE Cedex
FRANCE

ABSTRACT

The 3D active vision system illustrated in this paper has been developed for a geometrical study of object surfaces. Indeed, all our work has been directed towards the geometrical exploitation of the calculated 3D data. This is the reason for which the projected grid is considered as a network of curves rather than a graph.

In order to calculate the 3D coordinates we must first calibrate the camera and the projector. An original calibration system is proposed in this paper which calibrates the projector from the camera and permits to avoid the manual measurement of the 3D projected grid. The features of our calibration system are the efficiency, the autonomy, the precision of the reference data calculus, and the speed in calculating the system parameters.

Another important contribution of our work is the correspondence problem solving. Different from other published methods, the correspondence is done curve per curve without any ambiguity by using geometrical and global constraints. Thus, with the help of our 2D and 3D methods, all the 3D curves on the object surfaces can be calculated and not only the grid nodes.

Finally, the two families of 3D curves provided by our system allow us to calculate easily the shape parameters by using the concepts of differential geometry.

1- INTRODUCTION

In the recent years, 3D vision system using a structured light have widely been used in computer vision. The simplest projects a single spot and requires a bidirectional angular scanning in order to parametrize the object surface. The most common projects a laser plane which provides one parameter of the surface and the second parameter is defined indirectly. Moreover a very dense map must be computed in order to use Monge patch. Contrary to previous methods the grid projection provides two independent families of 3D curves which parametrize the object surfaces [GUI87] [GUI91] [STO86].

Our 3D active vision system using a grid have been developed for a geometrical study of surfaces. This is the reason for which all our 2D and 3D proposed methods are based on curve idea. The 2D methods used in the imaged grid extraction and which compose the first level of our 3D active sensor will be discussed briefly in section 3. For more details see [GUI87][GUI92].

Obtaining accurate three-dimensional measurements from a 3D active vision system using a grid is a task requiring precise calibration and reliable matching between the imaged grid and the original grid.

The calibration system described in this paper has been developed particularly for an automatic and

metrological use. The optical apparatuses which compose our 3D active sensor are one (or more) camera and one projector, the camera calibration has been widely analysed notably in stereo-vision systems [FAU87] but with regard to active vision system using a projector, few works have been done in this area.

For the projector calibration the 3D reference data are the 3D projected grid nodes, in order to avoid all manual measurements of these data - source of mistakes - we propose, in section 4 an optical and autonomous method for the projector calibration.

The major problem of 3D active vision system projecting an entire grid of lines is the correspondence problem solving between the original and imaged grids. We propose in section 5 a reliable method for the correspondence: each imaged curve is labeled independently from the other curves by using global and geometrical constraints. Thus, all the 3D grid points can be calculated and not only the grid nodes.

Our 3D sensor provides two families of 3D curves and permits to tackle easily a geometrical study of object surfaces. This third level of our system will be discussed in section 6.

2- THE SYSTEM ARCHITECTURE

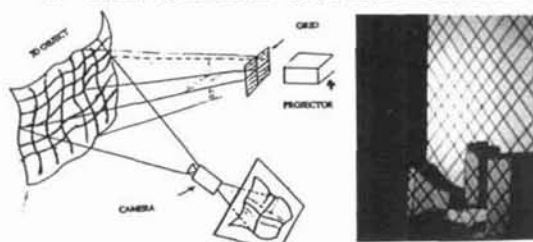


figure 1(a): sensing environment

figure 1(b): image of scene with the projected grid

figure 1: 3D active sensor

The proposed system consists of the following three levels:

- 1) **First level** : 2D processings (filtering, skeleton and imaged grid extractions)
- 2) **Second level** : 3D processings (calibration, correspondence, 3D reconstitution)
- 3) **Third level** : geometrical study of object surfaces (surface parametrization, shape parameter computations)

In view of the lower level importance in the comprehension of the developed 3D methods, we give a brief description of this level.

3- 2D PROCESSING

We describe the imaged grid with the highest precision. In order to do this, we carry out an efficient filter DRF [SHE86]. The extracted contours from the laplacian binary image are smoothed and 1 thick

connected skeleton is obtained by using an algorithm based on a distance function.

Once the intersection points (or nodes) of grid curves are detected, we extract the imaged grid curve per curve by using a directional procedure.

We reconstitute the imaged grid from the extracted curves. Thus, we obtain a segmentation of the imaged grid in connected components.

This level has been developed in order to extract as much as possible the 3D information on object surfaces.

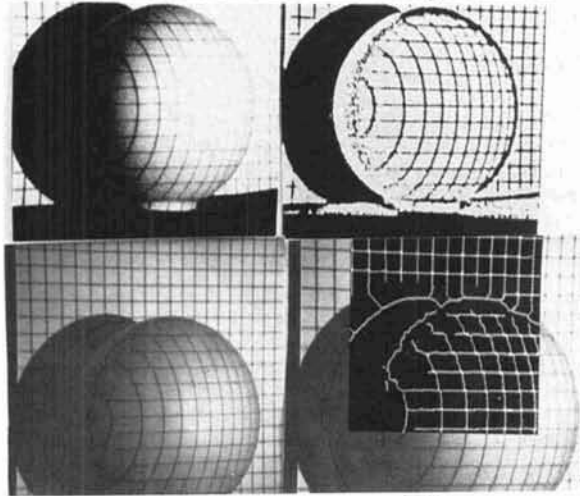


figure 2: 2D processing



where: figure2(a) is the initial image, figure 2(b) is the filtering result, figure2(c) is the skeleton and image2(d) shows the extracted curves.

4- CAMERA AND PROJECTOR CALIBRATIONS

The calibration of a 3D active vision system consists of computing both intrinsic and extrinsic parameters of the projector and the camera. This operation is necessary, on the one hand to solve the correspondence problem between the imaged grid nodes and the original grid nodes, and on the other hand to reconstitute the 3D scene.

The most frequently used approach existing in the bibliography [FAU87] consists of computing the perspective transformation matrix from where the camera parameters are derived by using the properties of the rotation matrix. The disadvantage of this approach is on the one hand the indirect calculus of the camera parameters from the projector transformation matrix coefficients, and on the other hand the equations allowing this calculus are non linear and very sensitive to errors. Indeed, it has been shown that a small error in the calculated coefficients of the perspective transformation matrix (due to the noisy 2D and 3D data) induces an important error on the derived camera parameters and above all on the calculation of the intrinsic parameters.

Contrary to the previous approach, our method is rather vectorial. In our case, the perspective transformation matrix is not explicitly computed but the camera parameters (extrinsic and intrinsic) are calculated directly from a recursive succession of linear systems.

In the remaining of this paper, vectors are denoted by bold characters.

a) Coordinate systems

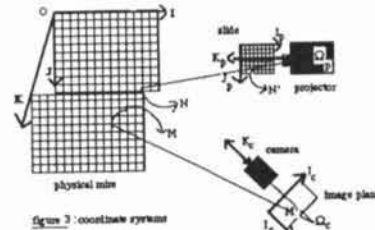


figure 3 : coordinate systems

Where:

- (O, I, J, K) is the world coordinate systems

- $(\Omega_c, I_c, J_c, K_c)$ is the CCD camera orthonormal repere such that: Ω_c is the camera optic center at a distance f_c of the image plane, (I_c, J_c) is the image plane and K_c is the camera optic axis (the digitized image is 512 x 512 pixels).

- $(\Omega_p, I_p, J_p, K_p)$ is the projector orthonormal repere such that: Ω_p is the projector optic center at a distance f_p of the grid plane, (I_p, J_p) is the grid plane (slide) and K_p is the projector optic axis.

b) Reference data

- The camera calibration pattern is a grid of lines drawn with a laser printer lying on 2 planes (physical mire) and a 3D calibration point is determined as the intersection of two lines.

- The projector calibration pattern is a grid of lines drawn on a transparent support (slide).

The projector calibration necessitates the knowledge of the 3D projected grid (optical mire) nodes. In practice, it is hard to measure manually the 3D coordinates of the

projected grid with a high precision. In order to avoid all manual measurements and to get the system more practical and precise, we propose to calibrate the projector from the camera. So, we use a slide grid with an orientation of 45° and we proceed in 4 stages:

1) we calibrate the camera by using the physical mire (figure 4(a))

2) We project the original grid onto the mire planes.(figure4(b))

3) We calculate the 3D projected grid (optical mire) from the camera parameters and the imaged grid.

4) We calibrate the projector from the original grid nodes and the calculated 3D projected grid.

The calibration precision depends on the precision of the reference data: physical and optical mire nodes, imaged nodes and slide grid nodes.

- Physical mire and the slide grid are provided with a precision of 0.1 mm and 0.01mm respectively.

- Imaged grid node computations: from the image of the two superimposed grids (the mire and the projected grids (figure 4(b)), we have to extract and to recognize the two grids in the image. In order to do this, we have developed a reliable method which calculate mathematically with the highest precision the imaged grid nodes of both physical and optical mires

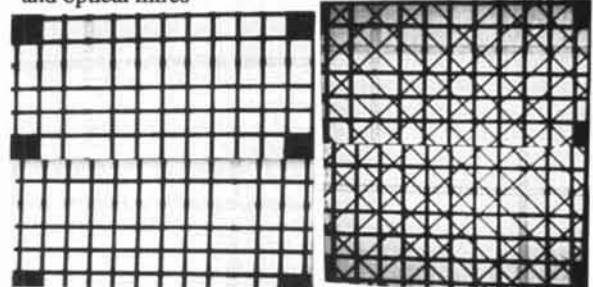


figure 4(a): physical mire

figure 4(b) : optical mire

c) Problem formulation

We assume that the camera and the projector perform a perfect perspective transformation with center Ω_c and Ω_p respectively. So, by using vectorial geometry we get the relationship between:

- a 3D space point M and its corresponding image M' :

$$\Omega_c M' = \frac{f_c}{(\Omega_c M, K_c)} \Omega_c M \quad (1) \quad [(.) = \text{inner product}]$$

- and a 2D projected grid node N' and its 3D projection

$$N: \Omega_p N' = \frac{f_p}{(\Omega_p N, K_p)} \Omega_p N \quad (2)$$

Projecting the relationship (1) onto the vectors I_c and J_c and expressing the resulting relationship in both world repere and camera repere we get for the camera the following system:

$$\begin{cases} i_c^k - \alpha_c = \frac{f_c/k_x [(OM^k, I_c) - (O\Omega_c, I_c)]}{[(OM^k, K_c) - (O\Omega_c, K_c)]} \\ j_c^k - \beta_c = \frac{f_c/k_y [(OM^k, J_c) - (O\Omega_c, J_c)]}{[(OM^k, K_c) - (O\Omega_c, K_c)]} \end{cases} \quad (S)$$

pour $k = 1, \dots, n$

where:

$\{M^k / k=1, n\}$ are the 3D reference points expressed in (O, I, J, K) and (i_c^k, j_c^k) the 2D coordinates of their corresponding images.

(α_c, β_c) are the 2D coordinates of the image origin (orthogonal projection of Ω_c onto the image plane).

k_x and k_y are the interpixel distances in the I_c and J_c directions

Likewise, we get from the relation (2) a similar system for the projector parameter computations.

d) Calibration system resolution

Our objective is to calculate a set of α_c and β_c values which converge on the correct image origin value. This convergence is assumed verified when K_c is perpendicular to the vectors I_c and J_c . In order to do this, we propose to replace the non linear system (S) by a succession of linear systems $(S)^{(n)}$. The unknowns of each linear system are: $I_c, J_c, K_c, (O\Omega_c, I_c), (O\Omega_c, J_c)$ and $(O\Omega_c, K_c)$.

The main outlines of our technique are the following: Each linear system $(S)_n$ is derived from the system $(S)_{n-1}$ as follows: if $(I_c^{(n-1)}, J_c^{(n-1)}, K_c^{(n-1)})$ is the $(S)_{n-1}$ solution, then we get the system $(S)_n$ by setting: $\alpha_c^{(n)} = \alpha_c^{(n-1)} + (I_c^{(n-1)}, K_c^{(n-1)})$ and $\beta_c^{(n)} = \beta_c^{(n-1)} + (J_c^{(n-1)}, K_c^{(n-1)})$. We start with $\alpha_c^{(0)} = \beta_c^{(0)} = 0$. Each linear system is solved under the constraint $\|K_c\| = 1$ and the used numerical method is the pseudo-inverse.

5) Precision test

We test the precision of our calibration system on a polyedral reference object manufactured with a precision of 0.1mm. Our precision is of 0.7mm for a distance between the system camera-projector and the object of about 3.5 m.

In order to calculate the 3D coordinates from the 3D active vision system using a projected grid, we have to solve the correspondence problem which will be discussed in the following section.

5 - CORRESPONDENCE

The correspondence problem consists of establishing the link between the projected grid and the imaged grid. Different from other published

methods[STO86], the correspondence problem is solved curve per curve by using global and geometrical constraints.

Our method characteristics are the followings :

- The correspondence between an imaged grid curve and a projected grid line is done independently from the other curves .

- Each connected component imaged grid is labeled independently from other components. Thus, the hidden nodes can be detected .

- We do not have to distinguish between horizontal and vertical curves (curves resulting respectively from horizontal and vertical lines of the projected grid): this is done by the algorithm.

Let us define some notations:

- d_x (resp. d_y) denotes horizontal (resp. vertical) line of the projected grid.

- P_x (resp. P_y) denotes the plane defined by the projector focus Ω_p and d_x (resp. d_y) .

- M_x^i (resp. M_y^i) denotes the intersection between the camera ray $\Omega_c M_i$ (line from the camera focus Ω_c to the imaged node M_i) and the horizontal plane P_x (resp. the vertical plane P_y)

- $E_i = \{ M_x^i / x \text{ such that } \Omega_c M_i \cap P_x \neq \emptyset \}$ and

- $F_i = \{ M_y^i / y \text{ such that } \Omega_c M_i \cap P_y \neq \emptyset \}$

(\cap = intersection symbol)

- $M_i, M_{i+1}, \dots, M_{i+(n-1)}$ denote n consecutive nodes of the imaged grid curve (C)

Algorithm UCA (uniform correspondence algorithm)

For any imaged curve (C), we intend to find the corresponding line. Since this line may correspond to an horizontal or a vertical line, we do a search among the horizontal and vertical lines.

The algorithm consists of two stages :

1st stage : For the node M_i of the curve (C) we compute the quantities :

$$\|M_x^i M_{y_0}^i\| = \min_{M_y^j \in F_i} \|M_x^i M_y^j\| \text{ and } \|M_{x_0}^i M_y^i\| = \min_{M_x^j \in E_i} \|M_x^j M_y^i\|$$

2nd stage : We use the neighborhood constraints. Therefore, if we assume that the curve (C) corresponds to the line d_x and the node M_i is the image of $d_x \cap d_{y_0}$ then the neighbor M_{i+1} of M_i must correspond to $d_x \cap d_{y_{0+1}}$ (or to $d_x \cap d_{y_{0-1}}$) and so on. Thus, for the horizontal search , we associate at each d_x the sum U_x defined as follow :

$$U_x = \sum_{u=1}^{u=n-1} \|M_x^{i+u} M_{y_0+u}^{i+u}\| \text{ if } \|M_x^{i+1} M_{y_0+1}^{i+1}\| < \|M_x^{i+1} M_{y_0-1}^{i+1}\|$$

$$U_x = \sum_{u=1}^{u=n-1} \|M_x^{i+u} M_{y_0-u}^{i+u}\| \text{ if } \|M_x^{i+1} M_{y_0-1}^{i+1}\| < \|M_x^{i+1} M_{y_0+1}^{i+1}\|$$

Likewise, we associate at each vertical line of the projected grid the sum U_y :

$$U_y = \sum_{u=1}^{u=n-1} \|M_{x_0+u}^{i+u} M_y^{i+u}\| \text{ if } \|M_{x_0+1}^{i+1} M_y^{i+1}\| < \|M_{x_0-1}^{i+1} M_y^{i+1}\|$$

$$U_y = \sum_{u=1}^{u=n-1} \|M_{x_0-u}^{i+u} M_y^{i+u}\| \text{ if } \|M_{x_0-1}^{i+1} M_y^{i+1}\| < \|M_{x_0+1}^{i+1} M_y^{i+1}\|$$

Decision : The curve (C) corresponds to the horizontal line d_{x_0} if $U_{x_0} = \min_x (U_x)$ is less than $U_{y_0} = \min_y (U_y)$, and to the vertical line d_{y_0} else.

From the imaged curves λ_i and λ_m we reconstitute by triangulation the 3D corresponding curves Λ_i and Λ_m .

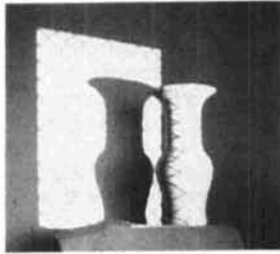


figure 5(a) : input image



figure 5(b) : binary image

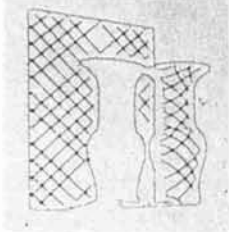


figure 5(c) : skeleton

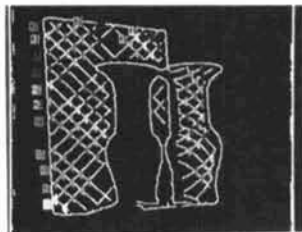


figure 5(d) : UCA result
(numbers show the corresponding lines)

Notice that - with the help of our 2D and 3D processings - all the 3D curves can be computed and not only the 3D grid nodes.

6- GEOMETRICAL INFERENCES

The interest of our system appears in the surface geometrical study. Indeed, we show that we can extract important information on the surface shape from a few 3D curves. In order to do this we first, define mathematically a parametrization of object surfaces.

a) Surface parametrization : The 3D calculated curves are necessary and sufficient to define mathematically the parametrization r of the surface region GP containing the 3D projected grid. Thus, GP is defined by: $\{ r(u,v) = [x(u,v), y(u,v), z(u,v)]$ where (u,v) moves along the 2 curve families λ_1 and λ_m . For more details see [GUI91].

b) Normal field computation: From the parametrization r we calculate the three fundamental vector fields for the surface geometrical study:

- 2 tangent vector fields X_1 and X_m such that :

$$X_1 : \Lambda_1 \rightarrow \mathcal{R}^3 \quad \text{and} \quad X_m : \Lambda_m \rightarrow \mathcal{R}^3$$

$$M \rightarrow (\partial r / \partial u)(M) \quad M \rightarrow (\partial r / \partial v)(M)$$

- the normal field n :

$$n : \Lambda_1 \cap \Lambda_m \rightarrow \mathcal{R}^3 \quad (x = \text{cross product})$$

$$M \rightarrow (\partial r / \partial u)(M) \times (\partial r / \partial v)(M)$$


figure 6(a) : depth map

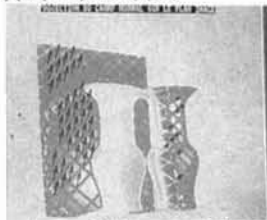


figure 6(b) : normal field

c) Surface curvatures: The surface shape depends on the normal vector field changing according to any tangent direction on the surface, this variation can be derived from the normal variation according to the curves Λ_1 and Λ_m . In order to calculate the surface curvatures we first, calculate the covariant derivative of the normal field according to any tangent direction on the surface. This covariant

derivative $\nabla_V n$ can be deduced from the normal variation according to the 3D curves Λ_1 and Λ_m :

$\nabla_V n = v_1 \nabla_{r'_1} n + v_2 \nabla_{r'_m} n$ with :

$$V = v_1 \frac{dr_1}{du}(Mo) + v_2 \frac{dr_m}{dv}(Mo) \quad (v_1, v_2) \in \mathcal{R}^2$$

$$r'_1 = \frac{dr_1}{du}(Mo) \quad \text{and} \quad r'_m = \frac{dr_m}{dv}(Mo)$$

Since the existing formulas of the Gaussian and mean curvatures from differential forms (connection and dual forms) in the literature can not be used under our hypothesis, we have been obliged to recalculate these curvatures from our parametrization by using Gauss-Godazzi formulas.

In order to calculate connection and dual forms, we define an orthonormal local repere (M, R_1, R_m, n) on the surface derived from the repere (M, r'_1, r'_m, n) . So, the calculated connections are the following differential forms ω_{31} and ω_{32} :

$$\omega_{31} : V \rightarrow f_1(Mo)dv_1(V) + f_2(Mo)dv_2(V)$$

$$\omega_{32} : V \rightarrow f_1(Mo)dv_1(V) + f_2(Mo)dv_2(V)$$

$$f_1 : M \rightarrow \nabla_{r'_1} n \cdot R_1 ; f_2 : M \rightarrow \nabla_{r'_m} n \cdot R_1$$

$$f_1 : M \rightarrow \nabla_{r'_1} n \cdot R_m ; f_2 : M \rightarrow \nabla_{r'_m} n \cdot R_m$$

$$dv_1 : (v_1, v_2) \rightarrow v_1 ; dv_2 : (v_1, v_2) \rightarrow v_2$$

And the calculated dual forms θ_1 and θ_2 :

$$\theta_1(V) = v_1 \sqrt{E_M} + v_2 \frac{F_M}{\sqrt{E_M}} ; \theta_2(V) = v_2(G_M - \frac{F_M^2}{E_M})$$

Where: E_M , F_M and G_M are the first quadratic form coefficients.

Finally, we get the following H and K formulas :

$$K = \frac{f_1 f_2 - f_2 f_1}{\sqrt{E_M} (G_M - \frac{F_M^2}{E_M})}$$

$$H = \frac{1}{2} \frac{\frac{F_M}{E_M} f_1 - f_2 \sqrt{E_M} - f_1 (G_M - \frac{F_M^2}{E_M})}{\sqrt{E_M} (G_M - \frac{F_M^2}{E_M})}$$

These formulas applied on the object in figure 2(a) show a plane surface (both Gaussian and mean curvatures are nearly zero) and an elliptical surface.

CONCLUSION

In conclusion, the results obtained from the experimental tests show the reliability of our methods based on the curve idea. The features of our system using a projected grid are its simplicity (the low cost in the system construction), its efficiency (the surface properties are calculated from curve fittings) and its precision (accurate system calibration).

REFERENCES

- [FAU87] = O.D. Faugeras and G.Toscani "Camera calibration for 3D computer vision" Proc.Int.Workshop Machine Vision & Match.Intell.Tokyo,Japan (1987)
- [GUI87] = L.Guisser "Système de Vision 3D Active à Paramétrization Directe de Surface" Thèse de 3ème cycle à l'UPS, Toulouse, FRANCE 1987
- [GUI91] = L.Guisser, R.Payrissat and S.Castan "A 3D Active Vision System with a Direct Paramétrization of Surfaces" SCIA '91, Aalborg, Denmark
- [GUI92] = L.Guisser, R.Payrissat and S.Castan "A New 3D Surface Measurement Using a Structured Light" CVPR'92, Champaign - Illinois, USA 1992
- [SHE86] = S.J.Shen and S.Castan "An Optimal Linear Operator for Edge Detection" CVPR'86, Miami 1986
- [STO86] = G.Stockman and G.Hu "Sensing 3D Surface Patches Using a Projected Grid" CVPR'86, Miami 1986